ResORR: A Globally Scalable and Satellite Data-driven Algorithm for River Flow Regulation due to Reservoir Operations

Pritam Das[1], Faisal Hossain[1], Sanchit Minocha[1], Sarath Suresh[1], George Darkwah[1], Hyongki Lee[2], Konstantinos M. Andreadis[3], and Perry C Oddo[4]

[1]University of Washington
[2]University of Houston
[3]University of Massachusetts Amherst
[4]Science Systems and Applications, Inc.

November 20, 2023

Abstract

Storage and release of surface water by reservoirs can alter the natural streamflow pattern of rivers with negative impacts on the environment. Such reservoir-driven river regulation is poorly understood at a global scale due to a lack of publicly available in-situ data on reservoir operations. However, with rapid advancements in satellite remote sensing-based tracking of reservoir state, this gap in data availability can be bridged. In this study, we modeled regulated flow of rivers using only satellite-observed reservoir state and hydrological modeling forced also with satellite precipitation data. We propose a globally scalable algorithm, ResORR (Reservoir Operations driven River Regulation), to predict regulated river flow and tested it over the heavily regulated basin of the Cumberland River in the US. ResORR was found able to model regulated river flow due to upstream reservoir operations of the Cumberland River. Over a mountainous basin dominated by high rainfall, ResORR was effective in capturing extreme flooding modified by upstream hydropower dam operations. ResORR successfully captured the peak of the regulated river flow altered by hydropower dam and flood control operations during the devastating floods of 2018 in the South Indian state of Kerala. On average, ResORR improved regulation river flow simulation by more than 50% across all performance metrics when compared to a hydrologic model without a regulation module. ResORR is a timely algorithm for understanding human regulation of surface water as satellite-estimated reservoir state is expected to improve globally with the recently launched Surface Water and Ocean Topography (SWOT) mission.

Hosted file

979200_0_art_file_11604954_s47ww8.docx available at https://authorea.com/users/701525/articles/687938-resorr-a-globally-scalable-and-satellite-data-driven-algorithm-for-river-flow-regulation-due-to-reservoir-operations

ResORR: A Globally Scalable and Satellite Data-driven Algorithm for River Flow Regulation due to Reservoir Operations

Pritam Das[1], Faisal Hossain[1*], Sanchit Minocha[1], Sarath Suresh[1], George K. Darkwah[1], Hyongki Lee[2], Konstantinos Andreadis[3], Miguel Laverde-Barajas[4] and Perry Oddo[5]

[1]Department of Civil and Environmental Engineering, University of Washington, Seattle, WA, USA

[2]Department of Civil and Environmental Engineering, University of Houston, Houston, TX, USA

[3]Department of Civil and Environmental Engineering, University of Massachusetts, Amherst, MA, USA

[4]Asian Disaster Preparedness Center, Bangkok, 10400, Thailand

[5]Science Systems and Applications, Inc., Lanham, MD, USA

* Corresponding Author.

Abstract

Storage and release of surface water by reservoirs can alter the natural streamflow pattern of rivers with negative impacts on the environment. Such reservoir-driven river regulation is poorly understood at a global scale due to a lack of publicly available in-situ data on reservoir operations. However, with rapid advancements in satellite remote sensing-based tracking of reservoir state, this gap in data availability can be bridged. In this study, we modeled regulated flow of rivers using only satellite-observed reservoir state and hydrological modeling forced also with satellite precipitation data. We propose a globally scalable algorithm, ResORR (Reservoir Operations driven River Regulation), to predict regulated river flow and tested it over the heavily regulated basin of the Cumberland River in the US. ResORR was found able to model regulated river flow due to upstream reservoir operations of the Cumberland River. Over a mountainous basin dominated by high rainfall, ResORR was effective in capturing extreme flooding modified by upstream hydropower dam operations. ResORR successfully captured the peak of the regulated river flow altered by hydropower dam and flood control operations during the devastating floods of 2018 in the South Indian state of Kerala. On average, ResORR improved regulation river flow simulation by more than 50% across all performance metrics when compared to a hydrologic model without a regulation module. ResORR is a timely algorithm for understanding human regulation of surface water as satellite-estimated reservoir state is expected to improve globally with the recently launched Surface Water and Ocean Topography (SWOT) mission.

Keywords

River Regulation, Reservoir Operations, Hydrological Modeling, Satellite Remote Sensing

Plain Language Summary: River flow that is regulated by upstream reservoir operations is difficult to model at a global scale without adequate parameterizations because of the lack of publicly available in-situ reservoir operation data. In this study, we developed a river flow regulation algorithm called ResORR that can be applied globally based entirely on satellite-based observation of reservoir states that are becoming now widely available. Tests over regulated river basins show that ResORR is able to improve the prediction of regulated river flow by at least

43 50% compared to the baseline of using a hydrologic model without a regulation or reservoir
44 module.

1. Introduction

46 Rivers have provided humans with food, water and energy security since human
47 civilization first started to take shape in ancient valleys of Tigris-Euphrates, Indus and Nile
48 rivers. This has only been made possible by means of control structures such as dams and
49 reservoirs, which allow storage and release of water from the river according to human needs.
50 Usually, water from the river is stored in reservoirs when the river naturally has higher flows,
51 resulting in a net reduction in the downstream flow of the river. This storage is driven by human
52 needs such as flood control or to meet future freshwater demand when natural availability may
53 be insufficient. The converse happens during naturally occurring periods of low flows, when
54 release of water from reservoirs artificially increases the downstream flow rate during the dry
55 season to meet demand for water. This regulation of surface water, in the form of alteration of
56 the streamflow from its natural pattern of discharge under pristine conditions, can be termed as
57 river regulation.

58 River regulation can change how the basin responds to a hydro-meteorological event in
59 the form of precipitation or snowmelt, affecting its natural variability and streamflow timing. For
60 instance, Wisser and Fekete (2009) found that the average residence time has increased by 42
61 days globally over the past century due to construction of reservoirs. Such disruption and
62 alteration of natural conditions is even more profound at a regional scale, for instance, Bonnema
63 and Hossain, (2017) note about 11-30% streamflow alteration in the Mekong basin, with the
64 residence time of reservoirs varying from 0.09 to 4.04 years. Vu et al., (2021) estimate that
65 reservoirs in the Mekong hold 50% of its dry season flow and 83% of its wet season flow. As a
66 result, the high flows of the Mekong-river have reduced by 31%, while the low-flows have
67 increased by 35%.

68 River regulation can also have serious ecological repercussions. For instance, the unique
69 annual flow reversal of the Tonle Sap River (TSR) leading to filling up the Tonle Sap Lake
70 (TSL) during the wet season and draining it during dry season may cease to exist if the flood
71 pulse of the Mekong River dampens by 50% and is delayed by a month (Pokhrel et al., 2018).
72 The absence of this unique flow reversal may have a negative impact on aquatic biodiversity,
73 particularly for fisheries and paddy planting (Marcaida et al., 2021). Similarly, in European
74 rivers, high-flows appear to be down by 10% while low-flows are up by 8% (Biemans et al.,
75 2011). Negative consequences are not limited to only ecological aspects but can also influence
76 the regional demand-and-supply of resources, with the potential to escalate pre-existing water
77 conflicts. The construction and filling up of the Grand Ethiopian Renaissance Dam (GERD) on
78 the Nile River has been a source of contention between Ethiopia and the other riparian countries
79 – Egypt and Sudan. Eldardiry and Hossain, (2021) estimate that if unprepared, the High Aswan
80 Dam (HAD) – a dam of existential importance to Egypt for its water-food-energy security – may
81 take anywhere from 2 years to 7 years to fully recover following the filling-up of the GERD.
82 Although, they also optimistically estimate that with cooperation and planning between the
83 riparian countries, the recovery period can be limited to immediate 2 years.

84 Apart from the direct alteration of streamflow timing of rivers, regulation due to dam and
85 reservoir operations can have an indirect effect on other components of the eco-system. For

86 instance, river regulation disturbs the natural sediment flow, resulting in a net reduction in
87 sediment deposition along shorelines of rivers, estuaries and oceans (Dunn et al., 2019; Li et al.,
88 2021). River water temperature anomalies owing to thermal stratification in reservoirs have also
89 been widely recognized (Ahmad et al., 2021; Cheng et al., 2020). Considering the sensitivity of
90 aquatic life to the water temperature changes (Caissie, 2006), river regulation can negatively
91 affect the environmental suitability for aquatic organisms (Cheng et al., 2022). Such negative
92 environmental consequences are a direct result of human decisions – which many consider
93 necessary to support the demands of a rapidly growing population. A better understanding of
94 human regulation of river flow, exacerbated by a changing climate and increasing freshwater
95 demand, is urgently required to ensure a sustainable future.

96 The coupled nature of human-water resources has led to developments in explicitly
97 modeling reservoir operations in Large-Scale Hydrological Models (LHMs) and Global
98 Circulation Models (GCMs) (Hanasaki et al., 2018; Wada et al., 2017). Existing methods to
99 represent human activities in hydrological models rely on modeling the optimal reservoir release
100 based on operating parameters such as the design role of the reservoir (Hanasaki et al., 2006),
101 land-water management schemes, downstream demand for water and energy (Alcamo et al.,
102 2003; Biemans et al., 2011; Haddeland et al., 2006; Vanderkelen et al., 2022). Many of these
103 human activities are often assumed or 'parameterized' due to lack of sufficient observational
104 data on reservoir operations. Using such a parameterized approach, Zhou et al. (2016) found that
105 in highly regulated basins, such as the Yellow and the Yangtze rivers, the seasonal reservoir
106 storage variations can contribute up to 72% of the variability of the basin's total storage. While
107 such key insights can be obtained using generic schemes of reservoir operations, the underlying
108 assumption of optimal reservoir operations may not always hold true. Stakeholders and reservoir
109 managers must often deviate from optimal operating conditions based on a variety of reasons,
110 such as adapting to regional water and energy demands, new hydro-political reality,
111 environmental regulations, and changing weather and climate patterns that result in river flow to
112 exceed the bounds of pre-dam historical flow records.

113 In the past, modeling human decisions of reservoir operations using parameterizations or
114 criteria-based assumptions has been the primary way for characterizing river-regulation due to a
115 lack of publicly available observations on dam operations. However, to better understand river
116 regulation, which is representative of the intricacies of operation of individual reservoirs, we
117 need to characterize and quantify river regulation grounded in observations of reservoir
118 operations (Biswas et al., 2021; Das et al., 2022; Zhou et al., 2016). Earth observing satellites,
119 with their vantage of space and a multi-decadal record of observations on reservoir operations
120 now provide an opportunity to fill this data availability gap by inferring reservoir operations
121 from space (Bonnema & Hossain, 2017). Rather than relying on parameterized or criteria-based
122 assumptions of reservoir operations, we can now use actual observation-based reservoir
123 operations to quantify the regulation of flow in physical models. Because satellite observations
124 today can track the dynamic state of reservoirs comprising surface area, water surface elevation,
125 evapotranspiration losses, storage change and even outflow (Cooley et al., 2021; Hossain et al.,
126 2017; Lee et al., 2010; Okeowo et al., 2017; Zhao et al., 2022), there is now a stronger argument
127 to move away from assumptions and parameterizations in representing human flow regulation in
128 physical hydrologic models.

129 Satellites such as the Landsat, Sentinel, and Jason series have been extensively
130 monitoring hydrologically relevant aspects of the Earth's surface, such as surface reflectance and

elevation, at the global scale. For instance, Gao et al., (2012) were able to recreate storage variations of large reservoirs using observations from the Moderate Resolution Imaging Spectroradiometer (MODIS) satellite platform. Cooley et al., (2021) used NASA's ICESat-2 satellite observations of water level height to estimate that about 3/5th of the Earth's surface water storage variability takes place due to reservoirs. Moreover, the recently launched terrestrial hydrology-focused Surface Water and Ocean Topography (SWOT) satellite is now expected to improve the monitoring of surface water resources at an unprecedented scale and accuracy (Biancamaria et al., 2016). Together, these Earth-observing satellites provide an opportunity to independently track various aspects of the hydrological cycle, including reservoir operations (Bonnema & Hossain, 2017; Hossain et al., 2017).

Using such multi-sensor satellite data on surface water, we can now build comprehensive, distributed, and scalable modeling platforms to simulate reservoir-river systems. The Reservoir Assessment Tool (RAT) is one such modeling platform that can estimate reservoir fluxes, comprising inflow to the reservoir, storage change, evaporative losses and outflow, solely using satellite data and hydrological modeling (Biswas et al., 2021; Das et al., 2022). More recent developments have made it easier to monitor reservoirs using RAT, further democratizing the availability of surface water data at the granular level for regulated river systems (Minocha et al., 2023). This has allowed for both global and regional scale studies of the anthropogenic impact on terrestrial water storage (Biswas & Hossain, 2022) and floods (Suresh et al., 2023), especially in the regions of the world that lack a robust data collection and sharing infrastructure.

Considering the importance and urgency of an observations-driven understanding of river regulation, there is now a need to develop methods to quantify river regulation due to reservoir operations that can be scaled globally based on publicly and globally available satellite observables. The wide availability of satellite-based reservoir operations data will only keep increasing with the recent launch of the SWOT mission that is optimized for surface water tracking, particularly for lakes and reservoirs. Here, the multi-satellite observations used by RAT to estimate storage change (Das et al., 2022) can be directly used as observations to quantify river regulation, obviating the need to separately model reservoir operations based on parameterizations or operating assumptions, which can be both difficult and unrepresentative of actual reservoir operations. Given the availability of multi-decadal satellite observations of surface water that are now made widely accessible due to advancements in information technology, we are now uniquely positioned to predict regulated flow at a level of granularity that was not possible before. Estimation of river regulation grounded in observational data inherently represents the actual or likely decisions made by reservoir operators. The primary research question that this paper addresses is – *How can river regulation due to operation of reservoirs be formulated in a globally scalable format using primarily satellite observations?* The objectives of the paper are as follows –

1. To develop a globally scalable river-regulation algorithm based on satellite observables or satellite derived reservoir data for predicting the human regulation of surface water.

2. To investigate incorporation of the river-regulation algorithm in the RAT modeling platform for regulated rivers, and quantify its skill in capturing river flow regulation at a basin scale.

2. Study area and Data

2.1. The Cumberland River in Tennessee, US

The Cumberland River is highly regulated by a system of 10 major dams and reservoirs with varying primary use cases, making it one of the most heavily regulated basins. The United States Army Corps of Engineers (USACE) Nashville District, own and operate 10 such multi-purpose dam/reservoir projects on the Cumberland River, with the first dams being built in 1950s. These dams are used for hydropower generation, flood control, recreation, commercial navigation, public water supply, and fisheries and wildlife management – bringing in immense economic benefits to the region (Robinson, 2019). Figure 1 compares the daily discharge in the Cumberland River for two time-periods corresponding to unregulated conditions (1916-1920) and regulated conditions (2016-2020). The effect of regulation can be clearly seen in the figure, in the form of reduced range and variability in the discharge hydrograph. Studies suggest that such regulation has caused a sharp decline in the population and species variety of Mussels in the basin, which were plentiful when the river was unregulated (Neel & Allen, 1964; Tippit et al., 1995; Wilson & Clark, 1914). In addition to the highly regulated status of the basin, the availability of long periods of in-situ observational data from the operating agencies makes this basin an ideal test bed for investigating anthropogenic river regulation (Bonnet et al., 2015).
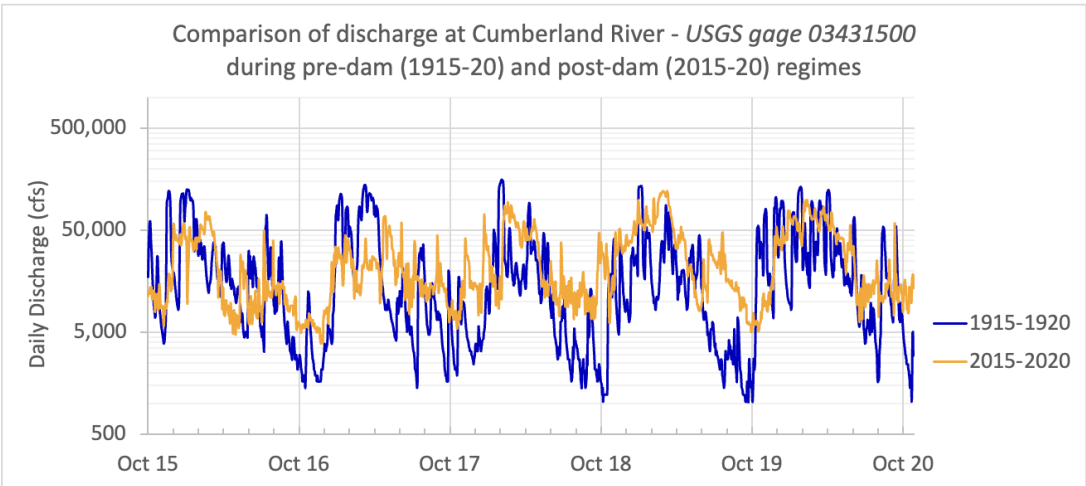

Figure 1: Comparison of 5 years of daily discharge during (a) unregulated conditions, prior to construction and operation of major dams (1916-1920), and (b) regulated conditions, as observed in the Cumberland River near Nashville, TN. The flow rate in a regulated regime has a markedly attenuated peak-trough range – with low flows rarely dropping below 5000 cfs as compared to the unregulated regime when flow rates naturally used to drop to 1000 cfs. Source: United States Geological Survey (USGS).

Originating in the Appalachian Mountains, the Cumberland River flows westwards through the states of Kentucky and Tennessee in the United States, draining a region of about 18,000 sq. miles (~45,000 sq. km), before merging into the Ohio River. Ten dams – Martins Fork, Laurel, Wolf Creek, Dale Hollow, Cordell Hull, Center Hill, Old Hickory, J. Percy Priest, Cheatham, and Barkley dams – are operated by USACE, with some additional dams operated by the Tennessee Valley Authority (TVA) (Robinson, 2019). Limited by the availability of in-situ reservoir operations data, 8 of the USACE owned dams were included in this study. Based on the

205 conclusions of the study, the authors believe that the results are not affected by the exclusion of
206 the 2 USACE dams owing to their relatively insignificant (Martin's Fork dam) to no storage
207 (Cheatham dam). The region generally has a temperate, warm, and humid climate, with most of
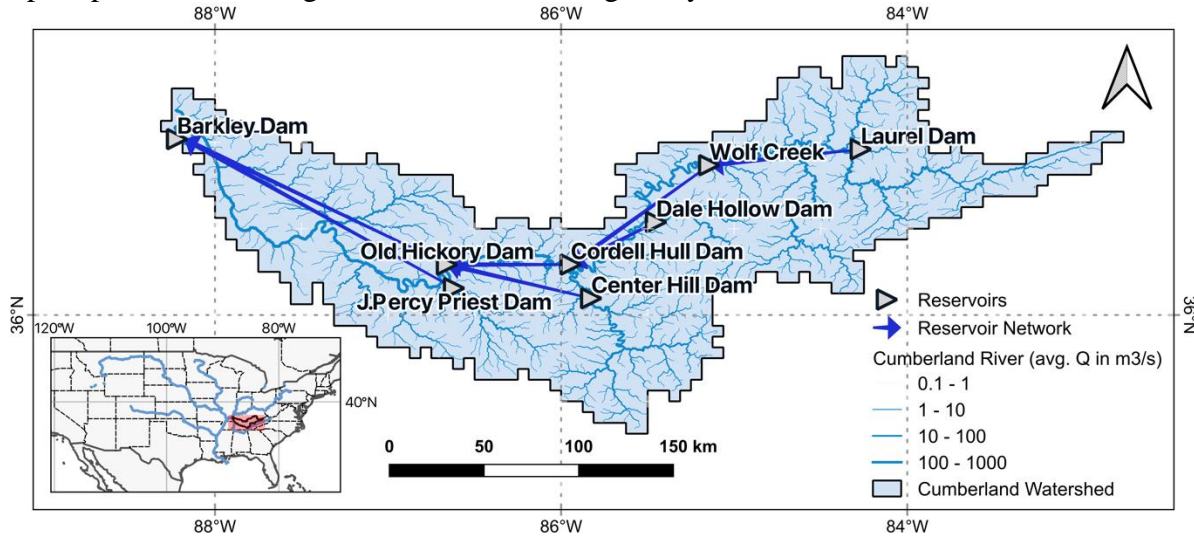208 the precipitation occurring from December through May.

209

210 Figure 2: Map of the Cumberland basin, showing locations of the reservoirs, the reservoir
211 network and the location of the Cumberland basin in the US.

212 2.2. In-situ and satellite observations of reservoir dynamics

213   To develop, test and validate the river-regulation algorithm, observed in-situ data
214 pertaining to reservoir operations – inflow, outflow, and storage – were used, which were
215 obtained from the ResOpsUS (Steyaert et al., 2022) dataset. This dataset is a compilation of in-
216 situ reservoir operations data for 679 major dams in the US, including 8 of the USACE dams in
217 the Cumberland basin and one dam operated by the TVA, until November 2019. Daily storage
218 change was calculated using the storage values in the dataset for all but 2 dams – Old Hickory
219 and J. Percy Priest – which had missing storage data from July 2015 onwards. The storage
220 change for these reservoirs were obtained by subtracting the reported Outflow from the Inflow
221 $(\Delta S = I - O)$. Readers are referred to section 8.2 for more discussion on this data preparation
222 step. The in-situ data was also used to force the river-regulation model in certain experiments to
223 compare the sensitivity of the river-regulation model to the accuracy of input data – a detailed
224 discussion is provided in section 4.1. Additionally, the in-situ Area-Elevation Curve (AEC) of all
225 the USACE reservoirs were also obtained from the Access to Water Resources Data – Corps
226 Water Management System (CWMS) Data Dissemination tool (USACE, n.d.).

227   The latest version of Reservoir Assessment Tool (RAT 3.0) was used to obtain the
228 storage change and river flow under pristine (naturalized) conditions (assuming no upstream
229 reservoirs). Originally developed by Biswas et al., (2021), the RAT framework is designed to
230 improve access to information on reservoir dynamics, especially with recent developments
231 leading to both a higher performance and accessibility (Das et al., 2022; Minocha et al., 2023).
232 Using the default hydrological model of RAT, Variable Infiltration Capacity (VIC) (Liang et al.,
233 1994), the inflow to each reservoir's location was estimated. The default VIC parameters, and
234 sources of temperature and wind data used in RAT 3.0 were used to force the hydrological

235 model. The precipitation was obtained from the ERA-5 reanalysis dataset (Hersbach et al.,
236 2020). It must be noted here that the VIC-based reservoir inflow in RAT 3.0 does not take
237 upstream reservoir operations into account, and hence the need to develop a model that can
238 supplement the RAT framework by taking upstream regulation into consideration. A detailed
239 discussion on how the hydrological model's estimated inflow in pristine conditions is used in the
240 river regulation model can be found in section 3.1. Since the in-situ AEC of the TVA-owned
241 reservoir was not available, the default AEC option in RAT 3.0 was applied based on the Shuttle
242 Radar Topography Mission Digital Elevation Model (SRTM DEM) (Earth Resources
243 Observation And Science (EROS) Center, 2017).

3. Methods

3.1. Reservoir Operations driven River Regulation (ResORR) – Conceptual algorithm

247 The core assumption of the ResORR algorithm is that the volume of water entering the
248 reservoir, Inflow (I), is composed of two components – natural and regulated. The Natural
249 Runoff (NR) is defined as the component of surface runoff that flows naturally into the reservoir
250 without passing through any upstream reservoirs. Similarly, the Regulated Runoff (RR) is the
251 component of surface runoff that first gets intercepted by an upstream reservoir before being
252 released based on the reservoir's operations policy. The partitioning of the inflow to a reservoir
253 is defined by the following equation,

$$I = NR + RR \qquad (1)$$

254 Essentially, the problem of estimating the inflow at any reservoir is decomposed into the
255 two parts of estimating the natural and regulated components of the incoming streamflow. A
256 detailed discussion on estimating these sub-components of inflow is provided later in the section.
257 The estimated inflow to a reservoir in this scheme will, hence, be affected by regulation due to
258 upstream reservoir operations.

259 For example, consider the example of a two-reservoir system (A and B), where reservoir
260 B is downstream of reservoir A, depicted in the schematic in Figure 3(a). In this scenario, the
261 inflow at reservoir B would have contributions from the outflow of the upstream reservoir A in
262 the form of RR (i.e., $RR \neq 0$), in addition to the NR. On the other hand, since reservoir A has no
263 upstream reservoirs, the inflow to the reservoir would be fully natural, i.e., $RR = 0$ and $I = NR$.
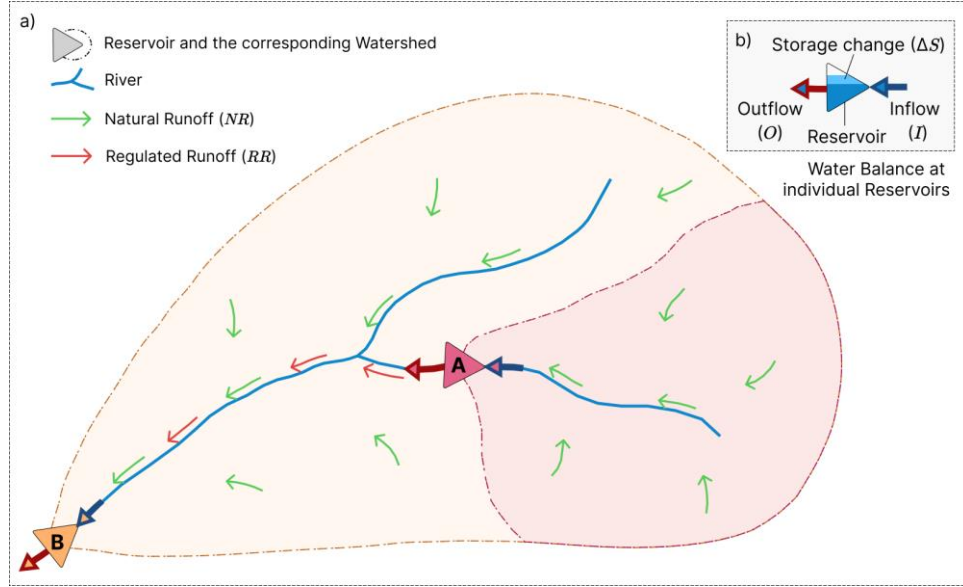
264
265 Figure 3: Conceptual schematic of the ResORR model. Panel (a) depicts the flow of surface
266 runoff and streamflow, along with the contribution of the natural (green arrows) and regulated
267 (red arrows along the stream) components, referred to in this paper as Natural Runoff (NR) and
268 Regulated Runoff (RR) to the Inflow ($I = NR + RR$) to a reservoir. Panel (b) describes the
269 components of the water balance equation ($O = I - \Delta S$) used at the reservoir to obtain the
270 outflow from the reservoir, which is treated as the regulated component of the downstream
271 streamflow.

272   As discussed above, the RR is defined as the component of inflow to a reservoir due to
273 upstream reservoir releases. It is estimated as the sum of all Outflow (O) of the upstream
274 reservoirs.

$$RR_i = \sum_j^N O_j \tag{2}$$

275   Where RR_i is the incoming Regulated Runoff to reservoir i; O_j is the Outflow from the
276 j^{th} upstream reservoir; N is the total number of upstream dams for reservoir i.

277   The NR is defined as the volume of water inflow to the reservoir due to surface runoff
278 unaffected by any upstream reservoir operations., i.e., the generated surface runoff drains
279 directly to the reservoir, without passing through any other reservoir. This surface runoff is
280 generated in the part of the watershed which is not shared by any other upstream dams. For
281 instance, in Figure 3, the orange and red shaded regions of the watershed will generate the NR
282 for reservoirs B and A respectively. The NR for a reservoir can be estimated using the theoretical
283 inflow into a reservoir if there were no upstream dams, which is referred to as the Theoretical
284 Natural Runoff (TNR) in this paper. The Theoretical Natural Runoff (TNR) refers to the inflow
285 to a reservoir if none of the upstream dams existed. The TNR can be calculated using the
286 following equation –

$$TNR_i = NR_i + \sum_j^N NR_j \tag{3}$$

287   Where, TNR_i is the Theoretical Natural Runoff of reservoir i; NR_i is the Natural Runoff
288   to reservoir i; and N is the total number of upstream dams of reservoir i along the same river
289   network. For example, in the schematic in Figure 3, the TNR of reservoir A and B would be NR_A
290   and $NR_B + NR_A$ respectively.

291   Since the TNR represents streamflow into a reservoir in pristine conditions (without
292   considering upstream reservoirs), it is analogous to the modeled inflow at reservoirs using
293   traditional hydrologic models which do not take reservoir operations into account. The NR of
294   any reservoir can be obtained by rearranging the terms of (3, and calculating the NR for
295   reservoirs by iteratively moving downstream for each time-step. The NR for any reservoir can
296   hence be obtained using the TNR of the reservoir, and the NR of the upstream reservoirs using
297   the following equation –

$$NR_i = TNR_i - \sum_{j}^{N} NR_j \tag{4}$$

298   Using the estimated NR and RR components, the inflow to a reservoir under regulated
299   conditions is then calculated using (1. Using the storage change of the reservoir, obtained either
300   in-situ or using satellite estimates, the outflow can then be calculated using the water balance
301   equation –

$$O = I - \Delta \tag{5}$$

302   Where O, I and ΔS are the outflow, inflow and storage change of a reservoir respectively. These
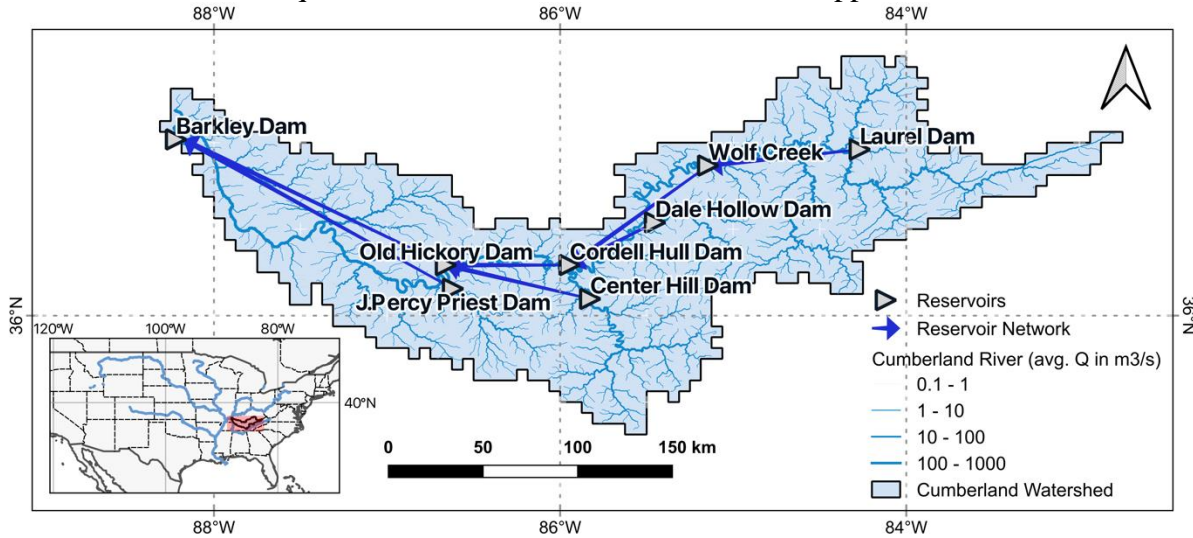303   equations were solved for the reservoirs mapped in

304

305   Figure 2 by traversing down the network of reservoirs for each time-step. To assess the
306   performance of the model, sensitivity to uncertainties in the model inputs, and generally
307   investigate the limitations of the model, various experiments were setup which are discussed in
308   section 4.1.

309   To test the theoretical robustness of the proposed river regulation algorithm as a mass
310   conserving scheme, we set up a two inter-connected linear reservoir problem where outflow is
311   proportional to water storage and according to the elevation head available at the outlet. Using
312   this set up we generated regulated inflow that should theoretically happen at the second reservoir

(reservoir 2) based on storage and regulation effect of the upstream reservoir (reservoir 1). Consequently, we tested the algorithm's ability to mimic the same regulated inflow to reservoir 2 using storage and upstream unregulated inflow of reservoir 1 that would be available in a globally scalable manner from satellite observations and modeling platforms such as RAT 3.0. Our algorithm demonstrated perfect theoretical consistency as a mass conserving scheme. More details on this theoretical robustness check of the algorithm are provided in the appendix (section 8).

3.2. Reservoir network

The reservoir network represents the connectivity of the reservoirs in the model and is represented by a directed tree data structure, with the nodes representing the reservoirs and the links depicting their connectivity, while preserving the order of reservoirs. The model first topologically sorts the reservoir network, to order them such that the water balance computations of upstream reservoirs are performed before the subsequent downstream reservoir. At each time-step, the model iterates over the topologically sorted reservoir network, and solves the series of equations discussed in 3.1.

The reservoir network is generated using the location of reservoirs and the Global Dominant River Tracing (DRT) dataset (Wu et al., 2011). Since the river-regulation model is designed as an add-on to the RAT framework, the script to generate the reservoir network can use the inputs and intermediary outputs of RAT to generate the reservoir network.

4. Experiments and Results

4.1. River regulation experiment setups using in-situ data

The ResORR algorithm is fully described by equations (1)-(5), which uses estimates of streamflow under pristine conditions from a hydrological model. However, the uncertainties in the estimations of hydrological model may propagate as uncertainty in the river-regulation model. Experiments were performed to isolate the performance of the core of the algorithm, its ability to partition the inflow between the natural and regulated components using in-situ observations in place of hydrological model and satellite estimates. By reducing uncertainties in certain parts of the algorithm, the performance of the individual components could be investigated, shedding light on the sensitivity of the algorithm components to the input data accuracy. Moreover, the observed in-situ ΔS was used in these experiments to gauge the baseline performance of ResORR using best available reservoir operations data, avoiding the higher uncertainties normally associated with satellite estimates of storage change.

To investigate the strengths and weaknesses of ResORR, especially in terms of scalability, the experiment designs were iteratively modified and updated in order from E1 to E4 over the period of 2015-2019. Details about the experiment designs and the rationale behind the experiments are summarized in Table 1.

Table 1: Summary of the experiments performed on the river regulation model along with the corresponding symbols used in the performance comparison plot (Figure 4).

Exp.	In-situ data used	Description	Rationale
E1 ○	ΔS	In-situ ΔS was used in eqn. (5) to estimate O. VIC hydrologic model was not calibrated for estimating natural inflow.	Uncertainties in satellite estimates of ΔS are minimized in this experiment.
E2 □	O	Observed O was used in eqn. (3) to estimate RR.	Uncertainties in otherwise estimated O, due to uncertainties in modeled I are minimized. The RR obtained as such would reflect the "theoretically" best estimate of incoming regulated streamflow.
E3 △	I, ΔS	Observed I was used in eqn. (4) only at the most upstream dam, where NR = TNR = I. In-situ ΔS was used in (5) to estimate O.	For upstream-most reservoirs all the incoming streamflow would be due to natural runoff, hence, by using the observed I, the uncertainties due to modeled I are minimized. The RR in this case would reflect the "theoretical best estimate" of the downstream regulated streamflow.
E4 ✚	ΔS	In-situ ΔS was used in eq (5) to estimate O. The VIC hydrological model, forced with satellite data, was calibrated at upstream most dams of Center Hill Dam, Dale Hollow Dam, and Laurel Dam.	The modeled inflow to the upstream most dams were calibrated using the observed inflow, essentially, minimizing the uncertainties at the upstream boundary of the reservoir network. This represents the ResORR in its globally scalable form under the scenario of perfect ΔS.

The regulated inflows obtained at the 4 dams, which have at least one upstream dam were compared against the observed inflow at those same dams. The comparison statistics measuring the performance of the river regulation model against observed inflow data are summarized in Figure 4. To understand how the river regulation algorithm is performing under various input scenarios and assumptions, one should compare the relative position of the symbols for each dam along the horizontal axis only. The TNR, obtained from the VIC hydrological model are denoted using grey and black circles, corresponding to the streamflow modeled using default parameter values and calibrated parameters. Formulation of performance metrics are provided in Appendix (section 8).
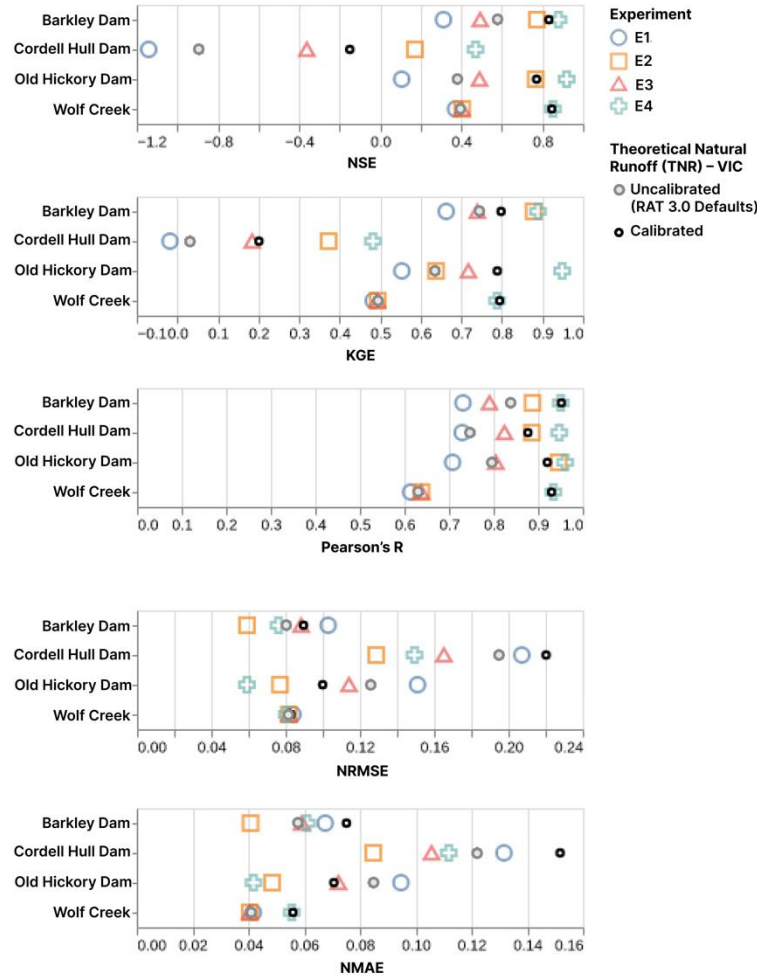
Figure 4: River regulation model performance for E* experiments using in-situ reservoir dynamics data.

Compared to the uncalibrated VIC streamflow estimates, the performance of the river regulation model in the E1 experiment in improving the accuracy of regulated inflow seems to be reduced. In other words, ResORR using in-situ ΔS, but with uncalibrated VIC flow at upstream most location does not improve the skill in predicted regulated inflow at downstream dam locations. However, on taking a closer look at the hydrographs comparing modeled inflow, TNR and observed inflow in Figure 5, it is apparent that the variability in the observed inflow, which is regulated inflow, is more closely replicated by the variability in the modeled inflow than the TNR. This likely suggests that even though the overall performance of ResORR gets reduced as a regulated streamflow predictor, the signature of human regulation is still captured well.

While analyzing the observed inflow hydrographs of two consecutive dams (Cordell Hull and Old Hickory dams) in Figure 6, a closer relationship between the downstream inflow and upstream outflow can be noted. It is clear that the upstream outflow plays a dominant role in dictating the downstream and regulated inflow at the next downstream dam as would be normally expected in the event of no lateral flow diversion. This relationship is further explored in the E2 experiment, where the daily in-situ outflow is used to calculate the RR to the downstream dam. Overall, the results improve across the board in the E2 experiment, underlining the role of upstream reservoir releases in predicting the downstream regulated streamflow. The

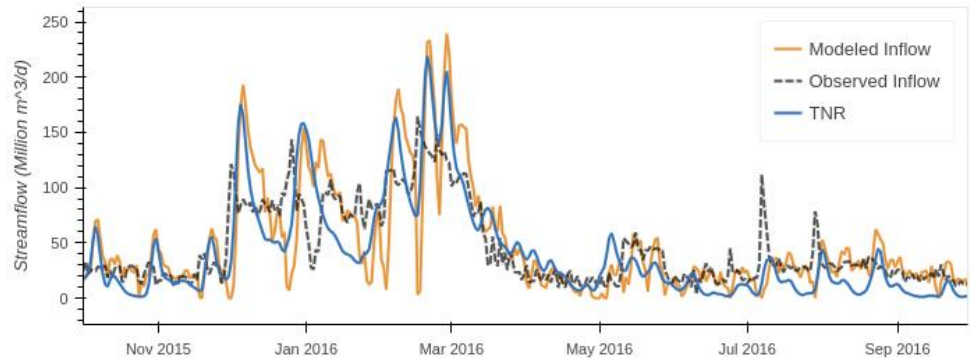E2 experiment also stresses the importance of having high accuracy estimates of reservoir storage data.

Figure 5: Hydrographs comparing the Modeled, Observed and TNR at Old Hickory Dam, which is the second most downstream dam in the network. The observed inflow is regulated inflow.

In the E3 experiment, the observed inflow to the upstream most dams was used as the NR. In most cases, the performance of the streamflow predictions still improved when adjusted for upstream regulation, as compared to the TNR. While this experiment suggests that if the accuracy of inflow estimates at the upstream most boundary conditions are accurate, that can improve the regulated streamflow estimates along that downstream network as well. Following this, the final E4 experiment, representative of the performance of the proposed and scalable river regulation model under accurate ΔS was performed. Here the VIC hydrological model was calibrated using the observed inflow at the upstream most dams. The result of this experiment shows the most significant improvement in the performance across all experiments. The performance of both the TNR, and the estimated regulated inflow improves in this case, nearly in all dams.
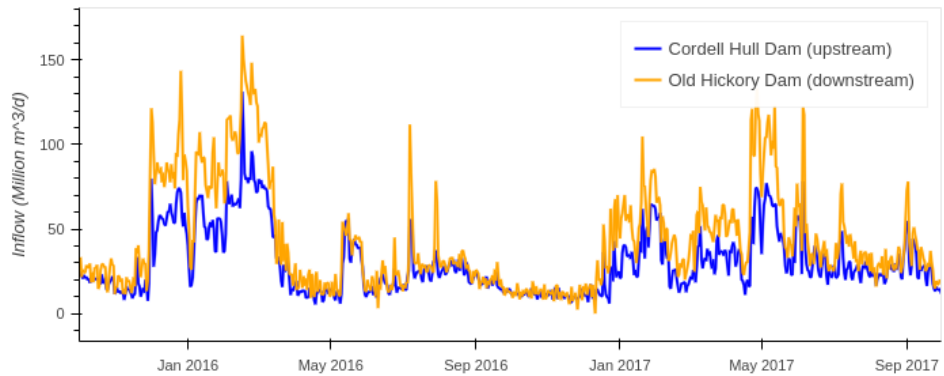

Figure 6: Observed inflows at two consecutive dams. The upstream Cordell Hull Dam drains into the downstream Old Hickory Dam, with the effect of upstream reservoir dynamics.

Moreover, the experiment results also shed light on the relationship between the model performance and the number of upstream dams. For instance, taking the case of the Wolf Creek dam (7.4 km^3 storage capacity), which only has one upstream dam (Laurel Dam, 0.5 km^3 storage capacity), the performance of the model does not improve as significantly as compared to the TNR. On the other hand, Cordell Hull Dam (run-of-the-river) is highly regulated and has two upstream dams, the Dale Hollow dam (2.1 km^3) and the Wolf Creek dam, and the performance of the streamflow estimates improves significantly by almost 50% across all the dams in the

406 basin. Overall, the results show that considering the effect of upstream regulation improves the
407 performance of the streamflow estimates at the downstream dams.

4.2. River regulation using satellite estimates of reservoir storage change

409 Now that E4 results established robustness of the proposed river regulation algorithm, we
410 explore how well ResORR fares with satellite-derived ΔS that will have higher uncertainty. The
411 inundation area of the reservoirs were obtained using the Landsat-8 and Sentinel-1 satellite data
412 from June 2018 to October 2021, using the TMS-OS algorithm described by Das et al., (2022).
413 The storage change of the reservoirs were then obtained using these surface area estimates and
414 in-situ Area-Elevation Curve (AEC), using the following equation –

415 $$\Delta S_t = \frac{A_t + A_{t-1}}{2} \times (h_t - h_{t-1}) \qquad (6)$$

416 Here the ΔS in equation 6 is the total volumetric storage change, A is the inundation area,
417 and h is the water level height corresponding to the inundation area, obtained using the AEC
418 relationship. The date of satellite observation is denoted by t, with $t-1$ referring to the last
419 satellite observation. For instance, since Landsat-8 has a revisit period of 16 days, the estimated
420 storage change would refer to the volumetric storage change within those 16 days. These storage
421 change estimates were transformed to daily values by linearly distributing the volumetric change
422 over 16 days. Based on the findings of the previous section, the VIC hydrological model was
423 calibrated at the upstream most dams, like the E4 experiment. The modeled inflow as such and
424 the streamflow estimates from VIC were compared against the observed in-situ inflow. The
425 results are summarized in Figure 7.

426 Similar to the results in the previous section, for the Cordell Hull and Old Hickory, both
427 run-of-the-river dams having upstream dams with large storage capacities, ResORR performance
428 increases significantly across all metrics. For the Wolf Creek dam, adjusting for the upstream
429 Laurel Dam's operations, ResORR performance does not increase as drastically, which can be
430 explained due to the relatively smaller size of the upstream Laurel Dam. Unlike the in-situ data-
431 based experiments, however, the model reduces the efficacy of inflow predictions for the
432 Barkley dam as compared to the TNR. This can be explained by the run-of-the-river nature of the
433 upstream dams, the storage change dynamics of which can be difficult to quantify using satellite
434 observations. Overall, the results suggest that river regulation due to dams can be characterized
435 by the proposed ResORR algorithm using satellite estimates of reservoir storage dynamics.
436 Adjusting for flow regulation due to upstream reservoir storage change improves the overall
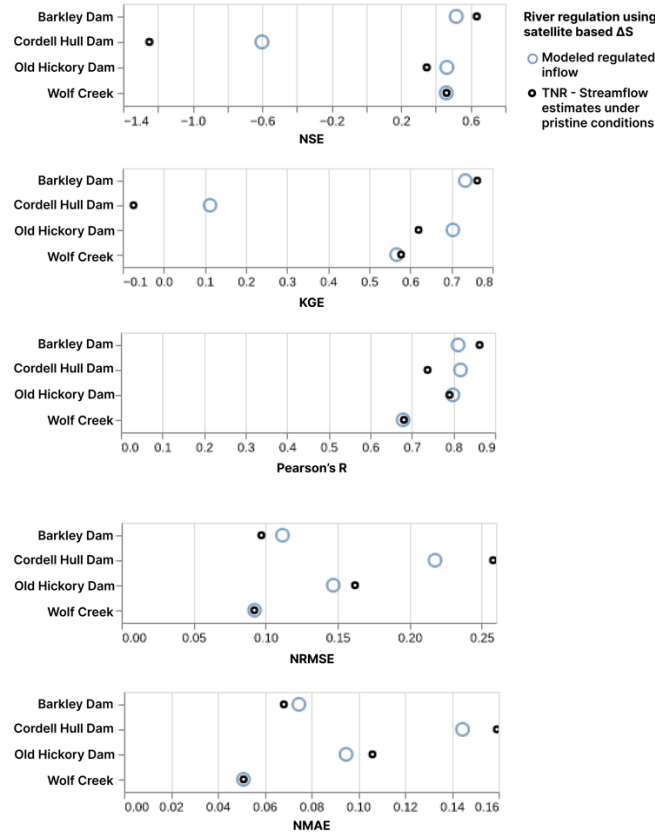437 inflow predictions in a regulated basin.

Figure 7: ResORR model performance using satellite derived reservoir storage change.

5. Scalability of ResORR - Case study of the 2018 floods in Kerala, India

In August 2018, the Indian state of Kerala experienced one of the worst cases of flooding in history due to an unexpectedly high precipitation event, which led to simultaneous release of water from 35 dams, leading to flooding at an unprecedented scale. The disaster claimed the lives of more than 480 people, displaced over 1.4 million and caused losses amounting to $5.0 billion (Suresh et al., 2023. The main driving force of the disaster was the extremely high precipitation, when from June 1, 2018 to August 19, 2018, a span of only three months, the state received 42% more precipitation than expected. The situation was made even worse by the unpreparedness of the dams to absorb the high inflow of water due to a lack of sufficient flood cushioning, as all the dams were operating on a rigid rule curve optimized for hydropower generation. The flood primarily affected the Periyar River basin which impacted the districts of Ernakulam, Kollam, Alappuzha and Kottayam (figure 8).

Most dams in the basin serve a dual purpose of hydro-electric power generation and flood moderation, which is intrinsically conflicting in nature. The role played by the upstream dam releases during the flooding of the basin and the basin's unique topographical and climatic characteristics make it a perfect case study for testing the scalability of ResORR using only satellite observations of reservoir state.
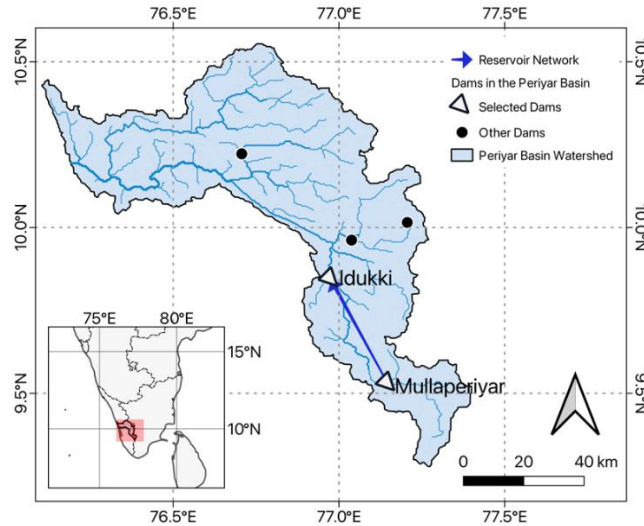
458
459 Figure 8: Map of the Periyar river basin showing the locations of Idukki and Mullaperiyar
460 reservoirs and the reservoir network.

461 RAT 3.0 was setup over the Periyar basin to obtain satellite estimates of reservoir
462 dynamics at a 1–5-day temporal frequency, including surface area and storage change estimates
463 from April 2018 to October 2018 using the TMS-OS algorithm. The reservoir network and the
464 TNR were obtained from the intermediary outputs of RAT 3.0. The VIC hydrological model
465 used in the RAT setup was also calibrated manually. The model was then run using the satellite-
466 observed reservoir dynamics and the modeled TNR. The hydrographs comparing the modeled
467 regulated inflow to the Idukki dam are shown in Figure 9. For more details on the RAT 3.0 set
468 up and the use of satellite observation for storage change estimation, readers are referred to
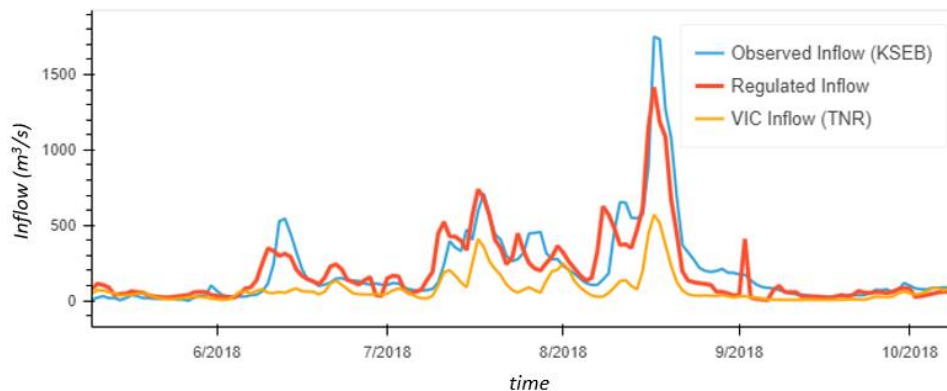469 Suresh et al. (2023).

470
471 Figure 9: Hydrographs comparing modeled regulated inflow from ResORR (red) and TNR
472 (orange as VIC inflow) against observed inflow (in blue as KSEB, which is regulated inflow) to
473 the Idukki dam during the 2018 floods. In-situ reservoir inflow data at Idukki dam provided by
474 Kerala State Electricity Board (KSEB).

475 Applying ResORR significantly improves the performance of the predicted inflow to the Idukki
476 dam as compared to just using VIC, which models streamflow under unregulated conditions. The
477 results also agree with the official reports, according to which large volumes of inflow was
478 received from the Mullaperiyar dam, leading to a rapid deterioration of the storage capacity of
479 Idukki, following which all 5 shutters of the dam were forced to be opened. The overall

480 prediction of downstream streamflow also improves drastically as evident from the comparison
481 metrics summarized in

482   Table 2. The performance of the streamflow predictions improves across the board,
483 especially the NSE and KGE metrics which improve significantly from 0.23 to 0.78 and 0.074 to
484 0.81, respectively. This demonstrates both, the important role played by the untimely release of
485 water from the upstream Mullaperiyar dam during the 2018 floods, and the ability of the
486 ResORR algorithm to correctly predict river regulation using only satellite observations.
487

488 Table 2: Statistics comparing the TNR and modeled inflow using ResORR against observed
489 inflow at the Idukki dam for the August 2018 Kerala floods.

	NSE	KGE	Pearson Correlation	Normalized RMSE	Normalized MAE
TNR	0.233	0.074	0.833	0.137	0.077
Modeled Regulated Inflow by ResORR	0.78	0.81	0.884	0.074	0.047

6. Conclusions and Discussion

491   Rivers of the 21st century are marked with numerous reservoirs, which store, and release
492 water based on their primary objectives, playing a vital role in providing food, water, and energy
493 security. However, such reservoir operations can alter the natural streamflow patterns, reducing
494 the water availability downstream by storing water during high flows, and *vice versa*. In this
495 study, we developed and tested a scalable and globally applicable river regulation model,
496 ResORR, to predict the regulation of streamflow due to upstream reservoir operations. Overall,
497 we find that adjusting for upstream reservoir operations via storage change improves the
498 accuracy of downstream streamflow predictions. The theoretical basis of the ResORR model was
499 tested using in-situ data in the heavily regulated Cumberland basin. The results stress the
500 importance of having high accuracy estimates of both the storage change and the hydrological
501 model. Moreover, we find that if the hydrological model can be calibrated for boundary
502 conditions of the reservoir network, *i.e.*, at the upstream most dams, significant improvement can
503 be achieved in predicting regulated inflow at all the downstream dam locations.

504   We also tested the scalability of ResORR by applying it over a completely independent
505 basin in Kerala, India. Using satellite observations alone, the model drastically improves the
506 downstream streamflow predictions. The role played by upstream reservoir releases during the
507 massive flood in 2018 that ravaged the entire state of Kerala was also captured by the model,
508 significantly improving the prediction of the timing and intensity of the flood peak that ravaged
509 the entire state of Kerala.

510   Currently, the reservoir network is automatically generated using the dam locations and
511 the DRT flow directions, and hence, any inter- or intra-basin diversions between reservoirs or
512 lateral diversions cannot yet be modeled. The regulation caused by reservoirs is also determined

by its storage capacity, and in a case where a small reservoir drains into a larger reservoir, the
algorithm adds little value to the streamflow predictions. Even with these limitations, the
ResORR algorithm can play an important role in quantifying the regulation of river flow due to
reservoirs in changing the world's river systems.

With advancements in satellite observations-based reservoir dynamics tracking,
especially the RAT 3.0, which has democratized access to reservoir operations information, it is
now possible to easily track the operations of reservoirs globally. Building on top of the RAT
framework, the proposed river regulation algorithm ResORR would also be able to characterize
the regulation of river flow using only satellite-tracked reservoir states at the global scale. The
ResORR software architecture is also designed to work seamlessly within the RAT framework,
i.e., it can run entirely using the RAT model outputs and intermediary files. With this river
regulation tool, the RAT framework will be able to not only infer reservoir dynamics, but also
quantify the regulation of streamflow caused by the upstream reservoir operations at the global
scale. We can expect ResORR to soon become a truly scalable algorithm based on the globally
available reservoir storage change data of unprecedent accuracy from the Surface Water and
Ocean Topography mission.

8. Open Research

Data Availability Statement
The Reservoir Assessment Tool (RAT) 3.0 (Minocha et al., 2023) was used to obtain satellite
estimates of unregulated streamflow estimates using its default options of models and datasets
(Bennett et al., 2020; Hamman et al., 2018, p. 5; Liang et al., 1994; Schaperow et al., 2021) for
reservoirs in both Cumberland and Kerala regions. The RAT 3.0 software with all documentation
and tutorials is available at http://ratdocs.io and https://www.satellitedams.net. The ResOpsUS
(Steyaert et al., 2022) dataset was used to obtain in-situ reservoir operations for reservoirs in the
Cumberland basin. The Dominant River Tracing (DRT) flow directions (Wu et al., 2012) were
used to generate the reservoir network. In-situ Area-Elevation relationships were digitized from
the Water Control Manual documents for reservoirs in the Cumberland basin from the Corps
Water Management System (CWMS) Data Dissemination repository. In-situ inflow data for
reservoirs in Kerala were digitized from reports on 2018 floods by the Kerala State Electricity
Board (KSEB). Compiled input data for running the ResORR model are available at zenodo
(10.5281/zenodo.10086338). The model code developed during this study is available on GitHub
(https://github.com/UW-SASWE/ResORR) under the MIT license. Documentation on ResORR
is available at - https://resorr.readthedocs.io/en/latest/?

555   **Author role:**

556   Research implementation: Pritam Das

557   Research design, data, and manuscript writing: Pritam Das and Faisal Hossain

558   Data, software and manuscript editing: Sanchit Minocha, George Darkwah and Sarath Suresh

559   Data and manuscript editing: Hyongki Lee and Konstantinos Andreadis

560   Research design and manuscript editing: Miguel Laverde-Barajas and Perry Oddo

7. References

Ahmad, S. K., Hossain, F., Holtgrieve, G. W., Pavelsky, T., & Galelli, S. (2021). Predicting the

    Likely Thermal Impact of Current and Future Dams Around the World. *Earth's Future*,

    9(10), e2020EF001916. https://doi.org/10.1029/2020EF001916

Alcamo, J., Döll, P., Henrichs, T., Kaspar, F., Lehner, B., Rösch, T., & Siebert, S. (2003).

    Development and testing of the WaterGAP 2 global model of water use and availability.

    Hydrological Sciences Journal, 48(3), 317–337.

    https://doi.org/10.1623/hysj.48.3.317.45290

Bennett, A., Hamman, J., & Nijssen, B. (2020). MetSim: A Python package for estimation and

    disaggregation of meteorological data. Journal of Open Source Software, 5(47), 2042.

    https://doi.org/10.21105/joss.02042

Biancamaria, S., Lettenmaier, D. P., & Pavelsky, T. M. (2016). The SWOT Mission and Its

    Capabilities for Land Hydrology. *Surveys in Geophysics*, 37(2), 307–337.

    https://doi.org/10.1007/s10712-015-9346-y

Biemans, H., Haddeland, I., Kabat, P., Ludwig, F., Hutjes, R. W. A., Heinke, J., von Bloh, W., &

    Gerten, D. (2011). Impact of reservoirs on river discharge and irrigation water supply

    during the 20th century. *Water Resources Research*, 47(3).

    https://doi.org/10.1029/2009WR008929

Biswas, N. K., & Hossain, F. (2022). A Multidecadal Analysis of Reservoir Storage Change in

    Developing Regions. *Journal of Hydrometeorology*, 23(1), 71–85.

    https://doi.org/10.1175/JHM-D-21-0053.1

Biswas, N. K., Hossain, F., Bonnema, M., Lee, H., & Chishtie, F. (2021). Towards a global

    Reservoir Assessment Tool for predicting hydrologic impacts and operating patterns of

584   existing and planned reservoirs. *Environmental Modelling & Software*, 140, 105043.

585   https://doi.org/10.1016/j.envsoft.2021.105043

586   Bonnema, M., & Hossain, F. (2017). Inferring reservoir operating patterns across the Mekong

587   Basin using only space observations. *Water Resources Research*, 53(5), 3791–3810.

588   https://doi.org/10.1002/2016WR019978

589   Bonnet, M., Witt, A., Steart, K., Hadjerioua, B., & Mobley, M. (2015). *The Economic Benefits of*

590   *Multipurpose Reservoirs in the United States-Federal Hydropower Fleet.*

591   https://doi.org/10.13140/RG.2.2.15894.14400

592   Caissie, D. (2006). The thermal regime of rivers: A review. *Freshwater Biology*, *51*(8), 1389–

593   1406. https://doi.org/10.1111/j.1365-2427.2006.01597.x

594   Cheng, Y., Nijssen, B., Holtgrieve, G. W., & Olden, J. D. (2022). Modeling the freshwater

595   ecological response to changes in flow and thermal regimes influenced by reservoir

596   dynamics. *Journal of Hydrology*, *608*, 127591.

597   https://doi.org/10.1016/j.jhydrol.2022.127591

598   Cheng, Y., Voisin, N., Yearsley, J. R., & Nijssen, B. (2020). Reservoirs Modify River Thermal

599   Regime Sensitivity to Climate Change: A Case Study in the Southeastern United States.

600   *Water Resources Research*, 56(6), e2019WR025784.

601   https://doi.org/10.1029/2019WR025784

602   Cooley, S. W., Ryan, J. C., & Smith, L. C. (2021). Human alteration of global surface water

603   storage variability. *Nature*, 591(7848), Article 7848. https://doi.org/10.1038/s41586-021-

604   03262-3

605   Das, P., Hossain, F., Khan, S., Biswas, N. K., Lee, H., Piman, T., Meechaiya, C., Ghimire, U., &

606   Hosen, K. (2022). Reservoir Assessment Tool 2.0: Stakeholder driven improvements to

satellite remote sensing based reservoir monitoring. *Environmental Modelling & Software*, 157(105533). https://doi.org/10.1016/j.envsoft.2022.105533

Dunn, F. E., Darby, S. E., Nicholls, R. J., Cohen, S., Zarfl, C., & Fekete, B. M. (2019). Projections of declining fluvial sediment delivery to major deltas worldwide in response to climate change and anthropogenic stress. *Environmental Research Letters*, *14*(8), 084034. https://doi.org/10.1088/1748-9326/ab304e

Earth Resources Observation And Science (EROS) Center. (2017). *Shuttle Radar Topography Mission (SRTM) 1 Arc-Second Global* [Tiff]. U.S. Geological Survey. https://doi.org/10.5066/F7PR7TFT

Eldardiry, H., & Hossain, F. (2021). A blueprint for adapting high Aswan dam operation in Egypt to challenges of filling and operation of the Grand Ethiopian Renaissance dam. *Journal of Hydrology*, 598, 125708. https://doi.org/10.1016/j.jhydrol.2020.125708

Gao, H., Birkett, C., & Lettenmaier, D. P. (2012). Global monitoring of large reservoir storage from satellite remote sensing. *Water Resources Research*, 48(9), 2012WR012063. https://doi.org/10.1029/2012WR012063

Gupta, H. V., Kling, H., Yilmaz, K. K., & Martinez, G. F. (2009). Decomposition of the mean squared error and NSE performance criteria: Implications for improving hydrological modelling. *Journal of Hydrology*, 377(1–2), 80–91. https://doi.org/10.1016/j.jhydrol.2009.08.003

Haddeland, I., Skaugen, T., & Lettenmaier, D. P. (2006). Anthropogenic impacts on continental surface water fluxes. *Geophysical Research Letters*, 33(8), L08406. https://doi.org/10.1029/2006GL026047

629   Hamman, J. J., Nijssen, B., Bohn, T. J., Gergel, D. R., & Mao, Y. (2018). The Variable

630   Infiltration Capacity model version 5 (VIC-5): Infrastructure improvements for new

631   applications and reproducibility. Geoscientific Model Development, 11(8), 3481–3496.

632   https://doi.org/10.5194/gmd-11-3481-2018Hanasaki, N., Kanae, S., & Oki, T. (2006). A

633   reservoir operation scheme for global river routing models. *Journal of Hydrology*, 327(1–

634   2), 22–41. https://doi.org/10.1016/j.jhydrol.2005.11.011

635   Hanasaki, N., Yoshikawa, S., Pokhrel, Y., & Kanae, S. (2018). A global hydrological simulation

636   to specify the sources of water used by humans. *Hydrology and Earth System Sciences*,

637   22(1), 789–817. https://doi.org/10.5194/hess-22-789-2018

638   Hersbach, H., Bell, B., Berrisford, P., Hirahara, S., Horányi, A., Muñoz-Sabater, J., Nicolas, J.,

639   Peubey, C., Radu, R., Schepers, D., Simmons, A., Soci, C., Abdalla, S., Abellan, X.,

640   Balsamo, G., Bechtold, P., Biavati, G., Bidlot, J., Bonavita, M., … Thépaut, J. (2020).

641   The ERA5 global reanalysis. *Quarterly Journal of the Royal Meteorological Society*,

642   146(730), 1999–2049. https://doi.org/10.1002/qj.3803

643   Hossain, F., Sikder, S., Biswas, N., Bonnema, M., Lee, H., Luong, N. D., Hiep, N. H., Du

644   Duong, B., & Long, D. (2017). Predicting Water Availability of the Regulated Mekong

645   River Basin Using Satellite Observations and a Physical Model. *Asian Journal of Water,*

646   *Environment and Pollution*, 14(3), 39–48. https://doi.org/10.3233/AJW-170024

647   Knoben, W. J. M., Freer, J. E., & Woods, R. A. (2019). *Technical note: Inherent benchmark or*

648   *not? Comparing Nash-Sutcliffe and Kling-Gupta efficiency scores* [Preprint]. Catchment

649   hydrology/Modelling approaches. https://doi.org/10.5194/hess-2019-327

650   Lee, H., Durand, M., Jung, H. C., Alsdorf, D., Shum, C. K., & Sheng, Y. (2010).

651   Characterization of surface water storage changes in Arctic lakes using simulated SWOT

652   measurements. *International Journal of Remote Sensing*, *31*(14), 3931–3953.

653   https://doi.org/10.1080/01431161.2010.483494

654 Li, S., Xu, Y. J., & Ni, M. (2021). Changes in sediment, nutrients and major ions in the world

655   largest reservoir: Effects of damming and reservoir operation. *Journal of Cleaner*

656   *Production*, 318, 128601. https://doi.org/10.1016/j.jclepro.2021.128601

657 Liang, X., Lettenmaier, D. P., Wood, E. F., & Burges, S. J. (1994). A simple hydrologically

658   based model of land surface water and energy fluxes for general circulation models.

659   *Journal of Geophysical Research: Atmospheres*, 99(D7), 14415–14428.

660   https://doi.org/10.1029/94JD00483

661 Marcaida, M., Farhat, Y., Muth, E.-N., Cheythyrith, C., Hok, L., Holtgrieve, G., Hossain, F.,

662   Neumann, R., & Kim, S.-H. (2021). A spatio-temporal analysis of rice production in

663   Tonle Sap floodplains in response to changing hydrology and climate. *Agricultural Water*

664   *Management*, 258, 107183. https://doi.org/10.1016/j.agwat.2021.107183

665 Minocha, S., Hossain, F., Das, P., Suresh, S., Khan, S., Darkwah, G., Lee, H., Galelli, S.,

666   Andreadis, K., & Oddo, P. (2023). *Reservoir Assessment Tool Version 3.0: A Scalable*

667   *and User-Friendly Software Platform to Mobilize the Global Water Management*

668   *Community* [Preprint]. Hydrology. https://doi.org/10.5194/gmd-2023-130

669 Nash, J. E., & Sutcliffe, J. V. (1970). River flow forecasting through conceptual models part I —

670   A discussion of principles. *Journal of Hydrology*, 10(3), 282–290.

671   https://doi.org/10.1016/0022-1694(70)90255-6

672 Neel, J. K., & Allen, W. R. (1964). The mussel fauna of the upper Cumberland Basin before its

673   impoundment. *Malacologia*, 1(3), 427–459.

674   Okeowo, M. A., Lee, H., Hossain, F., & Getirana, A. (2017). Automated Generation of Lakes

675   and Reservoirs Water Elevation Changes From Satellite Radar Altimetry. *IEEE Journal*

676   *of Selected Topics in Applied Earth Observations and Remote Sensing*, 10(8), 3465–

677   3481. https://doi.org/10.1109/JSTARS.2017.2684081

678   Pokhrel, Y., Shin, S., Lin, Z., Yamazaki, D., & Qi, J. (2018). Potential Disruption of Flood

679   Dynamics in the Lower Mekong River Basin Due to Upstream Flow Regulation.

680   *Scientific Reports*, 8(1), Article 1. https://doi.org/10.1038/s41598-018-35823-4

681   Robinson, J. A. (2019). *Estimated use of water in the Cumberland River watershed in 2010 and*

682   *projections of public-supply water use to 2040* (Report 2018–5130; Scientific

683   Investigations Report, p. 74). USGS Publications Warehouse.

684   https://doi.org/10.3133/sir20185130

685   Schaperow, J. R., Li, D., Margulis, S. A., & Lettenmaier, D. P. (2021). A near-global, high

686   resolution land surface parameter dataset for the variable infiltration capacity model.

687   *Scientific Data*, 8(1), 216. https://doi.org/10.1038/s41597-021-00999-4

688   Steyaert, J. C., Condon, L. E., W. D. Turner, S., & Voisin, N. (2022). ResOpsUS, a dataset of

689   historical reservoir operations in the contiguous United States. *Scientific Data*, 9(1),

690   Article 1. https://doi.org/10.1038/s41597-022-01134-7

691   Suresh, S., Hossain, F., Minocha, S., Das, P., Khan, S., Lee, H., Andreadis, K., & Oddo, P.

692   (2023). Satellite-based Tracking of Reservoir Operations for Flood Management during

693   the 2018 Extreme Weather Event in Kerala, India. *Remote Sensing of the Environment*

694   *(In review)* Available online at https://saswe.net/publications/RATKerala.pdf

695   Tippit, R. N., Brown, J. K., Sharber, J. F., & Miller, A. C. (1995). Modifying Cumberland River

696   system reservoir operations to improve mussel habitat. *Conservation and Management of*

Freshwater Mussels II: Initiatives for the Future. Proceedings of a UMRCC Symposium,

229–235.

USACE. (n.d.). *WM Data Dissemination*. Retrieved October 15, 2023, from

https://water.usace.army.mil/a2w/f?p=100:1:::::::#

Vanderkelen, I., Gharari, S., Mizukami, N., Clark, M. P., Lawrence, D. M., Swenson, S.,

Pokhrel, Y., Hanasaki, N., van Griensven, A., & Thiery, W. (2022). Evaluating a

reservoir parametrization in the vector-based global routing model mizuRoute (v2.0.1)

for Earth system model coupling. *Geoscientific Model Development*, 15(10), 4163–4192.

https://doi.org/10.5194/gmd-15-4163-2022

Vu, D. T., Dang, T. D., Galelli, S., & Hossain, F. (2021). Satellite observations reveal thirteen

years of reservoir filling strategies, operating rules, and hydrological alterations in the

Upper Mekong River Basin [Preprint]. Hydrology Earth System Science.

https://doi.org/10.1002/essoar.10507302.1

Wada, Y., Bierkens, M. F. P., de Roo, A., Dirmeyer, P. A., Famiglietti, J. S., Hanasaki, N.,

Konar, M., Liu, J., Müller Schmied, H., Oki, T., Pokhrel, Y., Sivapalan, M., Troy, T. J.,

van Dijk, A. I. J. M., van Emmerik, T., Van Huijgevoort, M. H. J., Van Lanen, H. A. J.,

Vörösmarty, C. J., Wanders, N., & Wheater, H. (2017). Human–water interface in

hydrological modelling: Current status and future directions. *Hydrology and Earth*

System Sciences, 21(8), 4169–4193. https://doi.org/10.5194/hess-21-4169-2017

Wilson, C. B., & Clark, H. W. (1914). *The mussels of the Cumberland River and its tributaries*

(Issue 781). US Government Printing Office.

Wisser, D., & Fekete, B. M. (2009). *Reconstructing 20th century global hydrography*.

719   Wu, H., Kimball, J. S., Mantua, N., & Stanford, J. (2011). Automated upscaling of river

720   networks for macroscale hydrological modeling: Upscaling f Global River Networks.

721   *Water Resources Research*, *47*(3).

722   Wu, H., Kimball, J. S., Li, H., Huang, M., Leung, L. R., & Adler, R. F. (2012). A new global

723   river network database for macroscale hydrologic modeling. *Water Resources Research,*

724   48(9), 2012WR012313.

725   https://doi.org/10.1029/2012WR012313https://doi.org/10.1029/2009WR008871

726   Zhao, G., Li, Y., Zhou, L., & Gao, H. (2022). Evaporative water loss of 1.42 million global

727   lakes. *Nature Communications*, 13(1), 3686. https://doi.org/10.1038/s41467-022-31125-6

728   Zhou, T., Nijssen, B., Gao, H., & Lettenmaier, D. P. (2016). The Contribution of Reservoirs to

729   Global Land Surface Water Storage Variations. *Journal of Hydrometeorology*, 17(1),

730   309–325. https://doi.org/10.1175/JHM-D-15-0002.1

731
732

8. Appendix

8.1. River-regulation in a theoretical two-reservoir system using synthetic data

A theoretical two inter-connected linear reservoir system with artificially generated headwater flow inputs was used to test the theoretical robustness of the mass conserving and numerical stability of the ResORR algorithm. This classic problem (Figure 10) also helped visualize the outputs of ResORR algorithm and verify if mass balance is maintained.
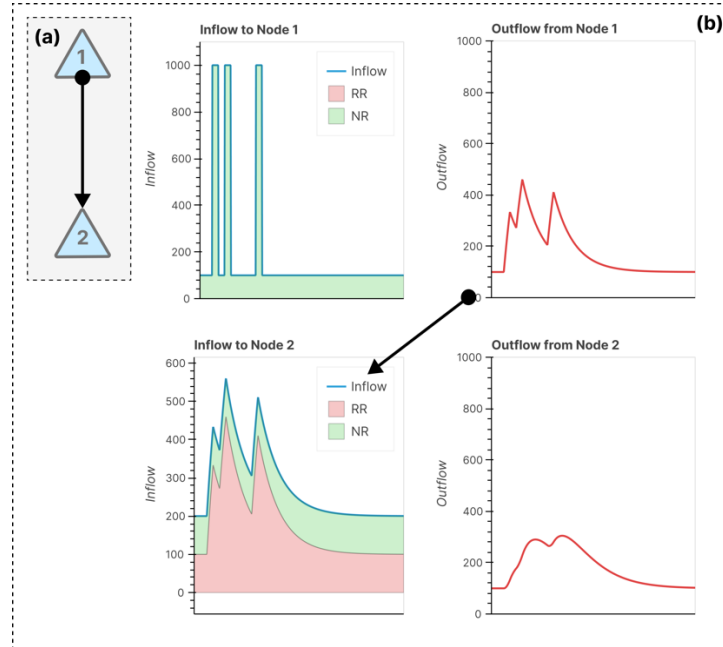

Figure 10: (a) Schematic showing the two-reservoir system setup. The black arrow denotes the direction of flow of water. (b) Hydrographs showing inflow and outflow from nodes 1 and 2. In this case, three input pulses of 1000 L^3/T units were fed into node 1, and its outflow was treated as the inflow to the downstream node 2. The inflow and outflow at node 2 represent the 'theoretical' answer for the ResORR algorithm to be theoretically valid.

A system of two interconnected linear reservoirs were set up, like the schematic shown in Figure 10. To understand how the outflow from an upstream reservoir would affect the inflow to the downstream reservoir, we first generated a synthetic headwater inflow hydrograph for reservoir 1and then applied ResORR to predict the regulated inflow to the downstream reservoir at node 2. Both the reservoirs were provided with a constant water influx of 100 L^3/T units in the form of natural runoff, NR. Additionally, the upstream reservoir, at node 1, was provided with three pulses of high inflow volumes of 1000 L^3/T units. The reservoirs were treated as linear reservoirs, where the outflow from a reservoir at any given time as a linear function of the instantaneous storage, and can be defined as follows –

$$O = K \times S$$

Where, K $[T^{-1}]$ is the reaction factor, which determines how quickly the reservoir drains ($K = 0.01$ in this experiment). The outflow from the upstream reservoir at node 1 was then treated as the regulated runoff, RR for the downstream reservoir, node 2. Using the inflows and

758 outflows obtained at both the reservoirs, the storage change was obtained using (5). The
759 theoretical natural runoff, TNR, was also obtained using (3). The ResORR was then run using
760 this simulated storage change and TNR information as inputs, to model the inflow at both the
761 reservoirs. The modeled inflow of ResORR was then compared with the synthetically generated
762 inflow at the downstream node 2, with a perfect match between them. The closure of water
763 balance was also tested by comparing the total inflow volumes in the modeled and synthetic
764 inflow.

8.2. Performance metrics used for assessing ResORR

766 The following five commonly used performance metrics were used in this study to
767 quantify the skill of the river regulation model -

Metric	Equation	Description
Nash-Sutcliffe Efficiency (NSE) (Nash & Sutcliffe, 1970)	$$1 - \frac{\sum_{t=1}^{T}(Q_O^t - Q_M^t)^2}{\sum_{t=1}^{T}(Q_O^t - \overline{Q_O})^2}$$ Where, Q_O^t and Q_M^t are observed and modeled streamflow respectively. $\overline{Q_O}$ is the mean observed streamflow.	The NSE can vary between $-\infty$ and 1. A value of 1 indicates a perfect match between observed and modeled values. A value of 0 indicates that the model predictions are as performant as using the mean of the observed values as a predictor. Higher values are better.
Kling-Gupta Efficiency (KGE) (Gupta et al., 2009)	$$1 - \sqrt{(r-1)^2 + (\alpha-1)^2 + (\beta-1)^2}$$ Where, r is the linear correlation between modeled and observed values, $\alpha = \left(\frac{\sigma_M}{\sigma_O} - 1\right)^2$, σ_M and σ_O are the standard deviations of the modeled and observed values, $\beta = \left(\frac{\mu_M}{\mu_O} - 1\right)^2$, μ_M and μ_O are mean modeled and observed values.	The KGE varies between $-\infty$ and 1. A value of -0.41 indicates model performance equal to using the mean of the observed values as a predictor (Knoben et al., 2019). Higher values are better.
Pearson's R	$$\frac{cov(Q_O, Q_M)}{\sigma_O \sigma_M}$$ Where, $cov(Q_O, Q_M)$ is the covariance of the observed and modeled values. σ_M and σ_O are the standard deviations of the modeled and observed values	The Pearson's R can vary from -1 to 1, where 1 indicates a perfect positive linear correlation. A value of 0 indicates no correlation.
Normalized Root-Mean Squared Error (NRMSE)	$$\frac{\sqrt{\frac{\sum_{i=1}^{N}(Q_O - Q_M)^2}{N}}}{\max(Q_O) - \min(Q_O)}$$ Where, $\max(Q_O)$ and $\min(Q_O)$ are the maximum and minimum observed	The NRMSE represents the standard deviation of the residuals as a fraction of the range of the observed values. Lower values are better.

	streamflow values.	
Normalized Mean Absolute Error (NMAE)	$$\frac{\frac{\sum_{i=1}^{N} |Q_M - Q_O|}{N}}{\max(Q_O) - \min(Q_O)}$$ Where, N is the number of observations, $|Q_M - Q_O|$ is the absolute difference of modeled and observed values	The NMAE represents the average absolute difference between observed and modeled values as a fraction of the range of observed values. Lower values are better.

8.3. Handling missing In-situ storage data

Two dams in the basin, Old Hickory and Laurel, had missing in-situ storage data after April 2015, due to which storage change could not be calculated using observed (in-situ) storage. This missing data was filled by assuming water mass-balance owing to inflow and outflow from the reservoirs, $\Delta S = I - O$.